



# Surface plasmon resonance device with imaging processing detector for refractive index measurements

Jimmy Castillo\*, Hector Gutierrez, Jose Chirinos, Jean Carlos Perez

Universidad Central de Venezuela, Facultad de Ciencias, Escuela de Química, Caracas, 1041A, Venezuela

## ARTICLE INFO

### Article history:

Received 5 November 2009

Received in revised form 1 June 2010

Accepted 3 June 2010

### Keywords:

Surface plasmon resonance

Refractive index measurement

## ABSTRACT

This work presents a new surface plasmon resonance (SPR) instrument based on Kretschmann configuration. This device acquires and processes the reflected SPR image of the sample by using a webcam together with an image processing algorithm that transforms the RGB image in numeric values and correlates the integrated intensity with the refractive index of the solution. Experimental signals were compared with theoretical values and it was found an excellent agreement. In addition, the applicability of the instrument was tested by measuring the refractive index of solutions in a continuous flow mode. Excellent stability and sensitivity of the signal were found in the presence of small changes of the refractive index.

© 2010 Elsevier B.V. All rights reserved.

## 1. Introduction

Surface plasmon waves can be excited on a thin metal film by light under a very narrow range of conditions determined by the coupling medium, refractive index, and thickness of adsorbed layers of the analyte. The use of the plasmon resonance has extensively grown since its initial observation by Wood in 1902 [1]. SPR is a phenomenon capable of detecting small changes in the refractive index of the surrounding area of a thin metallic film in real time [2]. That is, by detecting localized small refractive index shifts, a SPR-based sensor is able to quantitatively describe the interaction of molecules on thin metal film [3].

Liedberg et al. [4] demonstrated the potential benefits of SPR for biosensor purposes in 1983 by adsorbing immunoglobulin G (IgG) antibody layer over on the gold sensing film, resulting in the subsequent selective binding and detection of IgG [4]. Then, the phenomenon has been commercialized and it has been used extensively in biosensor for monitoring specific interactions and interfaces (i.e. antigen–antibody [5–11], receptor–ligand [12–15], hormone–receptor [16–21] and drug–protein [22–25] interactions) and as highly sensitive technique for monitoring physicochemical phenomena (i.e. chemical reactions, absorption, degradation, and protein hybridizations) associated with thin dielectric films.

The typical SPR instrument is based on the Kretschmann configuration [26]. In this system, a light source mostly from a laser, is used to excite surface plasmons by coupling, at a well defined angle, the p-polarized light from the laser into a prism, on which a thin gold or silver film is deposited. Recording the intensity of the reflected light as a function of the incidence angle of the light beam reveals a sharp

minimum at the plasmon angle  $\theta_p$  where the optimal coupling occurs between surface plasmon and incident light [27]. The performance of the system depends on the precision of this angle determination. The main limitation of this configuration is that it requires a high precision rotation mechanism to achieve a good resolution. To solve this issue, various schemes have been proposed which vary the wavelength of incident light, or utilize fiber optics and waveguides. In special, the use of SPR imaging has emerged as an effective method for qualitative and quantitative analysis of biological and chemical binding reactions. In these latter devices the collimated monochromatic light is reflected from the sensor surface in a typical Kretschmann configuration and focused onto a two-dimensional image detector and the generated signal is correlated with the refractive index of the sample. Chinowsky et al. [28] reported the construction and characterization of an imaging SPR instrument reaching approximately  $5 \times 10^{-7}$  RI measurement. Yu Xinlong [29] developed a SPR imaging interferometer for micro array detection to detect micro array chips in real time. Andrew [30] built a SPR imaging apparatus to detect Au coverage on patterned surfaces.

For all the above mentioned, the aim of this paper is to evaluate a new SPR device base on Kretschman configuration using a CCD detector together with a *Mathlab*<sup>®</sup> image processing algorithm. The main advantage of this new configuration is the possibility of recording the reflected signal without the necessity of any moving part of the instrument to register the signal. CCD detector permits the registration of changes in the laser light intensities due to SPR phenomena. Specifically, this study focuses on the comparison of the simulated signal generated by this system with experimental results. The theoretical study considers the main variables responsible for the surface plasmon resonance generation such as the refractive index of the media, the incidence angle of the laser beam and the gold film thickness. Finally, the applicability of the instrument is tested by using solutions having different refractive indices.

\* Corresponding author.

E-mail address: [jimmy.castillo@ciens.ucv.ve](mailto:jimmy.castillo@ciens.ucv.ve) (J. Castillo).

1.1. Principle

Surface plasmons are wave modes, which propagate along a thin metal layer sandwiched between two dielectrics. These waves appear from the coupling of an incident  $k$ -vector of the incident light with the surface  $k$ -vector producing the surface plasmons with a propagation vector,  $k_{sp}$ . This wave vector can be determined by solving Maxwell's equations for an interface separating a metal from a dielectric interacting with a p-polarized light [31]. The following equations show the propagation wave vector for a light beam with angle  $\theta$  and metal/glass interface:

$$k_x = \sqrt{\epsilon_0} \frac{\omega}{c} \sin(\theta) = k_{sp} = \frac{\omega}{c} \sqrt{\frac{\epsilon_1 \cdot \epsilon_2}{\epsilon_1 + \epsilon_2}}, k_{zi} = \sqrt{\epsilon_i \left(\frac{\omega}{c}\right)^2 - k_z^2} \quad (1)$$

where  $\epsilon_1$  and  $\epsilon_2$  are the complex dielectric constants of the glass prism and metal, respectively,  $\epsilon_0$  is the light permittivity in the vacuum  $c$  is the light rate in the vacuum and  $\omega$  the frequency of the incident light. Here  $k_z$  is imaginary and the electric field distribution at the metal surface can be expressed by  $E = E_0 \exp(i(k_x x - k_z z - \omega t))$ . The excited surface plasmons decay exponentially with the layer depth along the surface normal direction. These conditions, allows a penetration distance about 0.425 nm under the wavelength of 632.8 nm.

From the Fresnel's equations it is possible to calculate the reflectivity of the p-polarized incident light by the following equation [32]:

$$R = |r_{012}|^2, r_{012} = \frac{E_{ref}}{E_{inc}} = \frac{r_{01} + r_{12} e^{2i\delta}}{1 + r_{01} \cdot r_{12} e^{2i\delta}}, r_{ij} = \frac{\left(\frac{k_{zi}}{\epsilon_i} - \frac{k_{zj}}{\epsilon_k}\right)}{\left(\frac{k_{zi}}{\epsilon_i} + \frac{k_{zj}}{\epsilon_k}\right)} \quad (2)$$

where,  $\delta = k_{z2} d_2$  and  $d_2$  is the thickness of the metal thin-film layer.

These equations permit to calculate the dispersion relation and reflectivity at a metal/dielectric interface. Now, to have a two-dimensional

imaging of the SPR, it's necessary to introduce a spatial distribution of the incident beam. In the ideal diffraction limited wave it is possible to approximate the spatial behavior of the beam as a Gaussian using the next equation. This shows the complex amplitude of the Gaussian beam [33].

$$E(x, z) = E_0 \frac{w_0}{w(z)} \exp\left[-\frac{x^2}{w^2(z)}\right] \exp\left(-j\left(kz + k \frac{x^2}{R(z)}\right) - \zeta(z)\right) \quad (3)$$

where  $w(z) = w_0 [1 + (z_0/z)^2]^{1/2}$  is the beam width,  $R(z) = z [1 + (z_0/z)^2]$  is the wavefront radius of curvature,  $\zeta(z) = \tan^{-1}(z/z_0)$ ,  $z_0 = k_0 w_0^2$  is the Rayleigh range, and  $w_0 = (\lambda z_0 / \pi)^{1/2}$ .

With Eq. (3) it is possible to calculate the 2 dimensional intensity profile of the incident Gaussian beam and the correspondent changes in the incident beam due to SPR at plane  $z=0$ , when it is focused directly onto the detector. Assuming the incident field at a plane  $z=0$  has a Gaussian profile it can calculate the projection of the beam in a plane D located at a distance  $l$  from the plane of the image.  $x_{min} = l_0 \sin(q_i) - \frac{D}{2} \cos(q_i)$ ,  $x_{max} = l_0 \sin(q_i) + \frac{D}{2} \cos(q_i)$ ,  $y_{max} = -l_0 \cos(q_i) + \frac{D}{2} \sin(q_i)$ ,  $y_{min} = -l_0 \cos(q_i) - \frac{D}{2} \sin(q_i)$  where  $x$  and  $y$  are the relative positions of the pixels in the plane D. Fig. 1 shows a sketch of the coordinates' transformation. This equation allows the simulation of the intensity of the Gaussian beam projected in a plane after interacting with a metal/glass interface and can be calculated using the SPR signal as a function of variables such as metal properties (thickness, origin, etc), probe beam wavelength and angle, etc.

2. Experimental

2.1. Preparation of the sensing surface

The sensing surface consisted of a glass microscope slide covered with approximately 50 nm of gold film. Glass slide was cleaned with

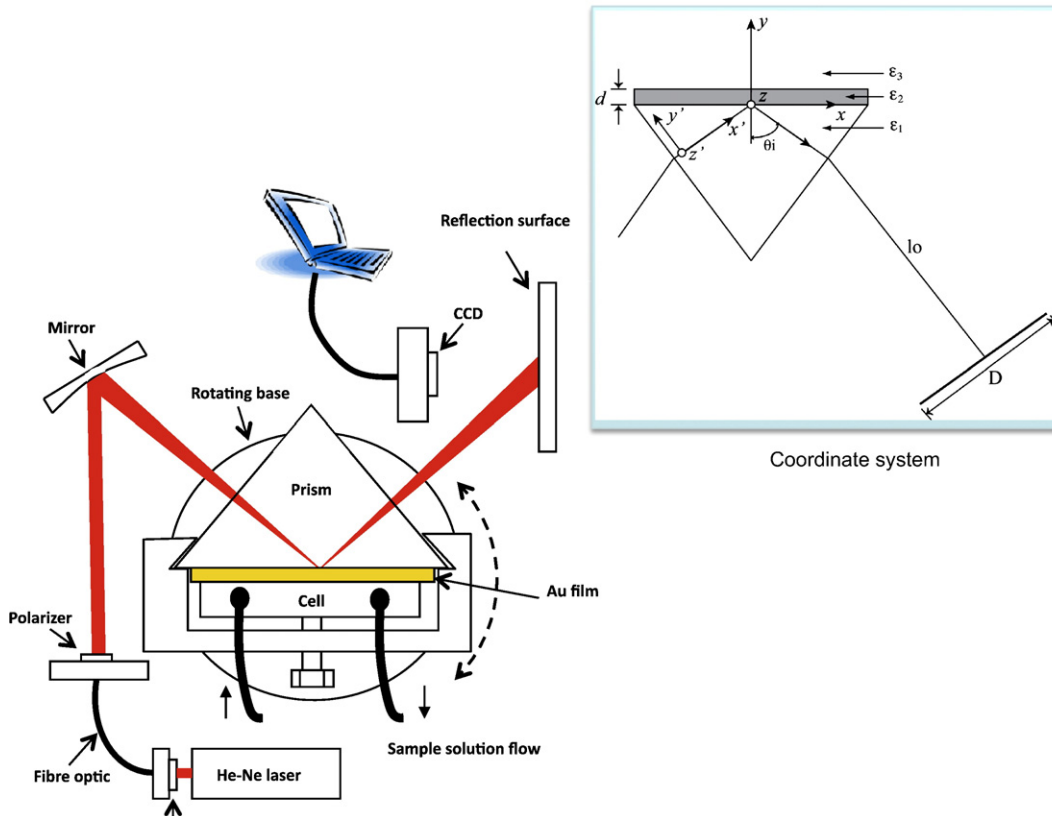


Fig. 1. Homemade SPR system setup.

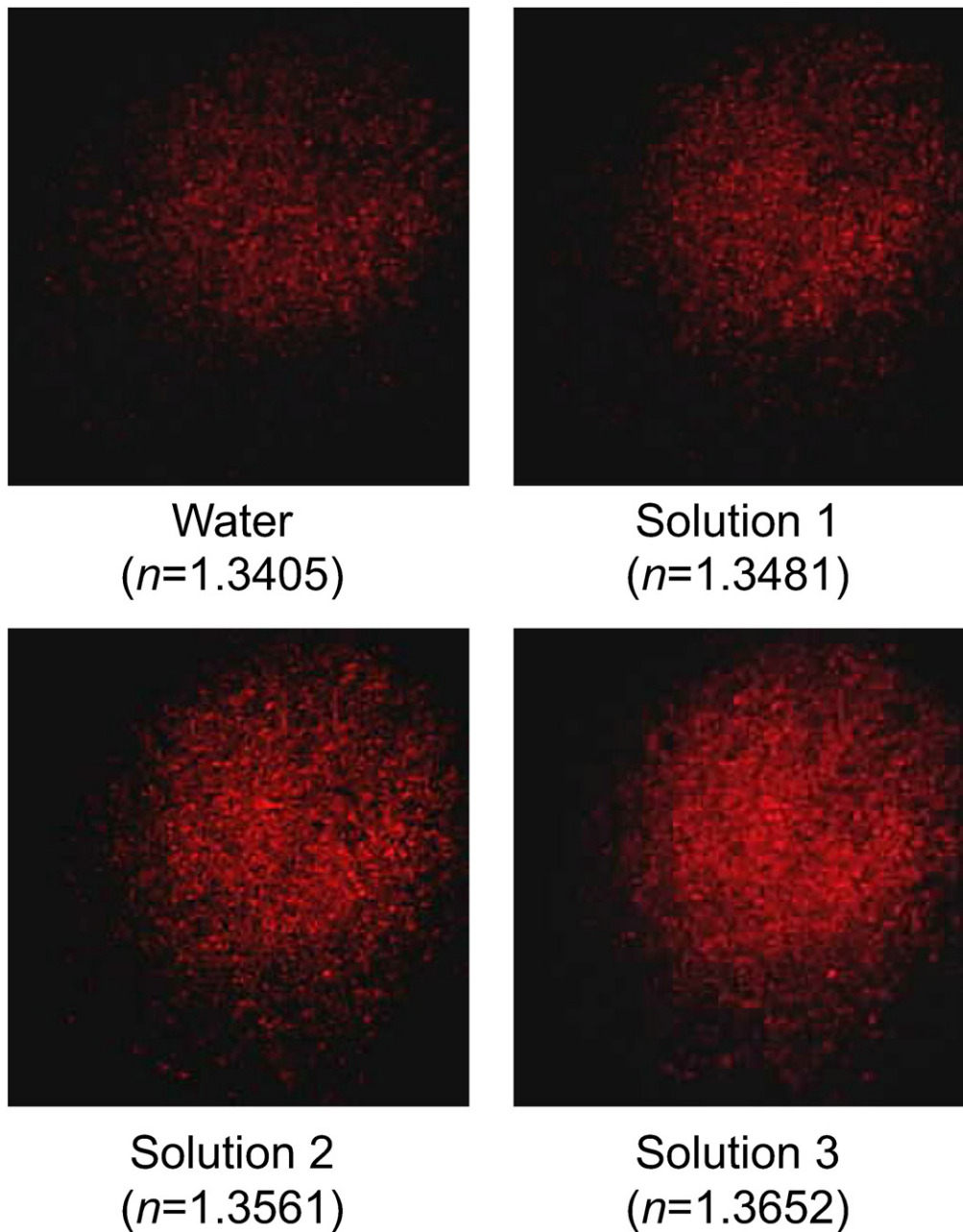


Fig. 2. Image reflected by the set up for two solutions with different refractive indices. A) Water ( $n = 1.3401$ ), B) Mixture water/ethanol ( $n = 1.3652$ ).

acetone and piranha solution (mixture of 3:1 concentrated sulfuric acid to 30% hydrogen peroxide solution) and coated with gold film by using a sputtering instrument (model Ion Coarter 2, Eiko Engineering, Ibaraki, Japan) under inert atmosphere conditions. The sputtering gas was argon. The thickness of the film layer was controlled by changing the time and intensity of the sputtering process. Atomic force microscope (model pico plus from Agilent) was used to measure the thickness of the sensing film.

## 2.2. Instrument

Fig. 1 presents the experimental set up used to obtain the surface plasmon resonance signal under Kretschmann configuration. The inset shows the reference coordinate system used to define the axis for the calculations. Glass slide with a 50 nm Au film is fixed to a right angle prism with immersion oil ( $n = 1.515$ , Merck, Germany). A continuous flow cell is attached to the prism–film system and adjusted with a screw.

The glass slide is in contact with the prism and the gold film with the liquid inside the flow cell. Light from a 5 mW He–Ne laser is guided to the set up by using 100  $\mu\text{m}$  multi-mode fiber-optic. In this configuration, the light is TM polarized and focused on the film at an incidence angle near to the critical angle where the total internal reflection is achieved. The liquid is forced through the continuous flow cell by using a peristaltic pump. The setup includes a rotating base for a coarse movement of the prism in order to set the angle of incidence at the maximum SPR effect. All the system is covered with isolated box to keep the temperature constant at 25  $^{\circ}\text{C}$ . The reflected beam is projected on a screen and a video of that image is recorded using a CCD camera (genius, model video Cam web V2) with 640  $\times$  480 pixels resolution at 20 frames/s.

The video is separated in frames and each frame is transformed in an intensity matrix using a *Mathlab*<sup>®</sup> (R2006a) algorithm. The images obtained by the camera have 3 components (RGB) the R channel with sensitivity to red color (wavelength from 580 nm to 700 nm), the G

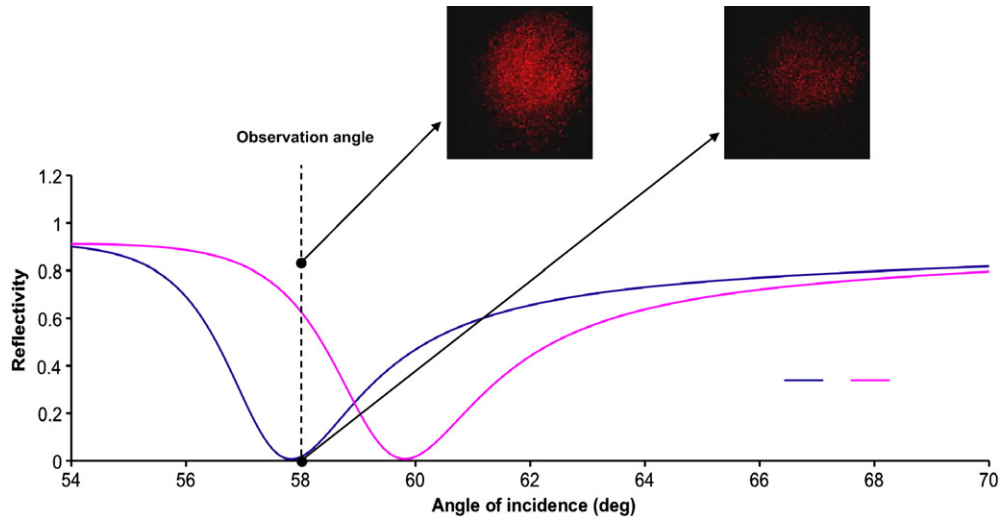


Fig. 3. Reflectivity as a function of the incidence angle.

channel with sensitivity to green color (wavelength from 450 nm to 600 nm) and the B with sensitivity to blue color (wavelength from 400 nm to 530 nm). The red channel of these images was selected and transformed into gray scale images. This transformation produces images composed by pixels with linear intensity values from 0 (black) to 255 (white). The reported intensity is the average of 30 frames. This procedure reduces the variability of the signal due to speckles in the image produced by the coherence of the laser. The reported intensity allows the detection of the SPR signal of samples having different refractive indices without any movement of the incidence angle or detector.

3. Results and discussion

3.1. SPR image analysis

The SPR integrated intensity mainly depends on three variables: the refractive index of the media, the incidence angle of the laser beam and the thickness of the gold film. The SPR signal as a function of these variables was calculated using Eq. (3). Fig. 2 shows the experimental images at fixed angle and film thickness of solutions having different refractive indices. This figure shows the increase of the intensity of the projected beam as the refractive index of the samples increases. This behavior is correlated well with the typical SPR behavior and it can be

explained with the sketch presented in Fig. 3, that shows a theoretical curve profile of the variations in reflectivity as a function of the incidence angle for two different samples. The minimum corresponds to the angle for maximum SPR signal. This can be related with the refractive index, if the measurement is taken at a fixed angle, as it was done in the experiment. The changes in the refractive index of the samples produce a relative change in the reflected intensity. The inset in Fig. 3 also shows the experimental images for samples of different refractive indices at a fixed angle. The reduction in the signal intensity is clearly produced by of the increase of the refractive index.

Fig. 4 presents the normalized integrated signal as a function of the refractive index for three gold film thickness: 45, 55 and 85 nm. The points are experimental values and the line is calculated using Eq. (3). According to this equation, the best fitting thickness values are 47, 60 and 70 nm. It can be appreciated that the sensitivity and linearity of the system depend strongly on the gold film thickness. This is because at this range of film thickness, the laser wavelength (632.8 nm) corresponds with the maximum in the surface plasmon resonance. For thicker gold films the plasmon resonance occurs at lower wavelengths. This effect is clearly observed for an 85 nm of film thickness, in this case the sensitivity is lower than that showed at 45 nm. These results demonstrate the applicability of the technique for the measurement of film thickness.

Fig. 5 presents the maximum variation in the integrated image for samples having different refractive indices measured in continuous

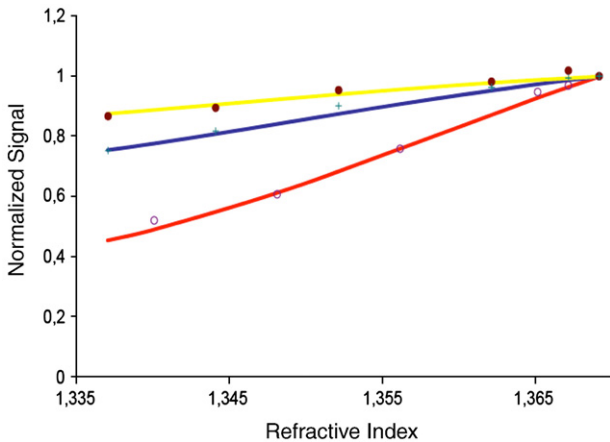


Fig. 4. Reflectivity normalized vs. refractive index obtained through system and by means of the simulation of a Gaussian beam for gold films with 45 (empty circles), 55 (cruz) and 85 (filled circles) nm of thickness. The lines are the best fitting curve using the Eq. (3).

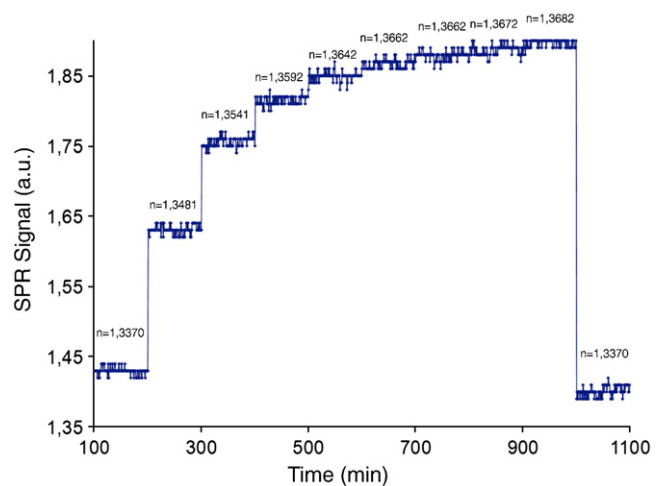


Fig. 5. SPR signal for mixtures with different refractive indices measured in continuous flow.

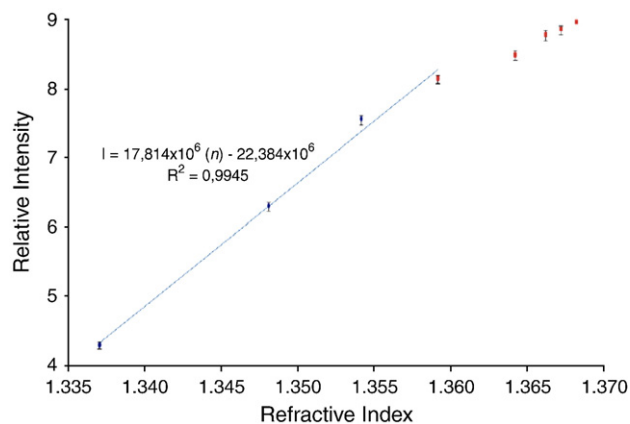


Fig. 6. Calibration curve of the system.

flow mode. First, it can be appreciated that the signal increases as the refractive index of the sample increases, with relative standard deviation (RSD) of 1.28%. Then the plot shows the increments of the signal followed by stability zones with very low variability. Finally, the signal recovers the initial value. It's important to note that the curve shows saturation at relatively higher refractive index values. This effect is a consequence of the reflectivity behavior presented in Fig. 2 where it is possible to appreciate that the increase of reflectivity is not linear with the refractive index. This phenomenon allows higher sensibility in a short lineal range. Fig. 6 shows a calibration curve of the relative intensity as a function of refractive index, the plot clearly exhibits two linear ranges with different sensitivities. The linear portion of the curve shows a correlation coefficient of 0.9945 and a linear range of 0.03 RIU. The slope of this curve corresponds to an analytical sensitivity of  $1.7 \times 10^{-5}$  RIU.

#### 4. Conclusions

This new simple and inexpensive design presented here demonstrates the advantage of an imaging system as a detector for SPR instrument. The system has the advantage of recording the reflected signal without the necessity of moving any part of the instrument. The study showed a good agreement between the theoretical description of the signal and the experimental results. It was found that there is a very good correlation, sensitivity and stability of the signal in the presence of small changes in the refractive index of the solutions.

#### Acknowledgement

This work was supported by Consejo de Desarrollo Científico y Humanístico CDCH-UCV through grant PG-03-00-5745-2004.

#### References

- [1] R.W. Wood, *Philosophical Magazine* 4 (1902) 396.
- [2] M.R. Aguilar, A. Gallardo, L.M. Lechuga, A. Calle, J.S. Roman, *Macromolecular Bioscience* 4 (2004) 631.
- [3] H. Jiri, S.Y. Sinclair, G. Gunter, *Sensors and Actuators B* 54 (3) (1999) 3.
- [4] B. Liedberg, C. Nylander, I. Lundstrom, *Sensors and Actuators B* 4 (1983) 299.
- [5] E. Tatsuuro, Y. Shohei, N. Naoki, M. Yasutaka, T. Yuzuru, T. Eiichi, *Science and Technology of Advanced Materials* 6 (491) (2005) 491.
- [6] J.W. Chung, S.D. Kim, R. Bernhardt, J.C. Pyun, *Sensors and Actuators B* 114 (2006) 1007.
- [7] S. Jung, H. Son, S. Yuk, J. Jung, K.H. Kim, C. Lee, H. Hwang, K. Ha, *Colloids and Surfaces: Biointerfaces* 47 (2006) 107.
- [8] K. Matsumoto, A. Torimaru, S. Ishitobi, T. Sakai, H. Ishikawa, K. Toko, N. Miura, T. Imato, *Talanta* 68 (2005) 305.
- [9] J.C. Pyun, S.D. Kim, J.W. Chung, *Analytical Biochemistry* 347 (2005) 227.
- [10] D.R. Shankarana, K.V. Gobia, T. Sakaic, K. Matsumoto, K. Tokod, N. Miurara, *Biosensors and Bioelectronics* 20 (2005) 1750.
- [11] D.S. Ri, K. Matsumoto, T. Ki, N. Miura, *Sensors and Actuators B* 114 (2006) 71.
- [12] J. Remy, C. Nespoulous, J. Grosclaude, D. Grebert, L. Coutre, E. Pajot, R. Sables, *Journal of Biological Chemistry* 276 (2001) 1681.
- [13] U. Sivaprasad, J.M. Canfield, C.L. Brooks, *Biochemistry* 43 (2004) (2004) 13755.
- [14] K. Hanada, H. Hirano, *Biochemistry* 43 (2004) 12105.
- [15] P. Prunet, O. Sandra, P.L. Rouzic, O. Marchand, V. Laudet, *Canadian Journal of Physiology and Pharmacology* 78 (2000) 1086.
- [16] D.M. Gakamsky, I.F. Luescher, Pecht, *PNAS* 101 (2004) 9063.
- [17] R.L. Rich, L. Hoth, K. Geoghegan, T.A. Brown, P.K. LeMotte, S.P. Simons, P. Hensley, D.G. Myszka, *PNAS* 99 (2002) 8562.
- [18] T. Fujino, Y. Sato, M. Uneb, T. Kanayasu-Toyoda, T. Yamaguchi, K. Shudo, K. Inoue, T. Nishimaki-Mogami, *The Journal of Steroid Biochemistry and Molecular Biology* 87 (2003) 247.
- [19] P. Pattnaik, *Applied Biochemistry and Biotechnology* 126 (2005) 79.
- [20] I.D. Alves, S.M. Cowell, Z. Salamon, S. Devanathan, G. Tollin, V.J. Hruby, *Molecular Pharmacology* 69 (2004) 1248.
- [21] J. Pearson, A. Gill, G.P. Margison, P. Vadgama, A.C. Povey, *Sensors and Actuators B* 76 (2001) 1.
- [22] R. Arnell, N. Ferraz, T. Fornstedt, *Analytical Chemistry* 78 (2006) 1682.
- [23] X. Liu, D. Song, Q. Zhang, Y. Tian, Z. Liu, H. Zhang, *Sensors and Actuators B* 117 (2006) 188.
- [24] H. Aizawa, M. Tozuka, S. Kurosawa, K. Kobayashi, S.M. Reddy, M. Higuchi, *Analytica Chimica Acta* 591 (2007) 191.
- [25] B. Fitzpatrick, R. O'Kennedy, *Journal of Immunological Methods* 291 (2004) 11.
- [26] E. Kretschmann, H. Raether, *Zeitschrift Naturforsch* 23 (1968) 2135.
- [27] F.C. Chien, S. Chen, J. Biosensors and Bioelectronics 20 (2004) (2004) 633.
- [28] M.T. Chinowsky, S.M. Grow, S.K. Johnston, K. Nelson, T. Edwards, E. Fu, P. Yager, *Biosensors and Bioelectronics* 22 (2007) 2208.
- [29] Y. Xinglong, W. Dingxin, W. Xing, D. Xiang, L. Wei, Z. Xinsheng, *Sensors and Actuators B* 108 (2005) 765.
- [30] L. Andrew Lyon, W.D. Holliday, M.J. Natan, *Review of Scientific Instruments* 70 (4) (1999) 2076.
- [31] K. Choi, H. Kim, Y. Lim, S. Kim, B. Lee, *Optics Express* 13 (2005) 8866.
- [32] N. Eum, S. Lee, D. Lee, D. Kwon, J. Shin, J. Kim, S. Kang, *Sensors and Actuators B* 96 (446) (2003) 4837.
- [33] J. Villatoro, A. Garcia-Valenzuela, *Applied Optics* 22 (1999) 4837.